

PRELIMINARY TESTING OF A TYPE III TAPERED-CYLINDRICAL GROUTED SEISMIC CONNECTOR FOR DUCTILE DEFORMED STEEL REBAR

Theresa C. Aragon, M.S., University of Notre Dame, Notre Dame, IN
Yahya C. Kurama, Ph.D., P.E., University of Notre Dame, Notre Dame, IN

ABSTRACT

This paper discusses the preliminary experimental results of a novel grouted Type III connector for ductile, energy-dissipating (ED) deformed reinforcing bars in gap-opening joints of seismic precast concrete structures (e.g., shear wall and column bases). The primary objective is to develop a high-performance, yet simple, non-proprietary, low-cost connector that allows ED bars under cyclic loading to reach close to their full ultimate strength and fracture strain capacity over a short cementitious-grouted embedment length of 10 times the bar diameter. The use of short grouted connections would simplify the construction of precast concrete structures because protruding bar lengths from precast members can be minimized and field grouting lengths can be reduced. The tested ED bars were subjected to a rigorous cyclic tension loading history inside a tapered-cylindrical grouted connector sleeve duct, and were able to sustain maximum strains close to the measured monotonic strain capacity of the bar at peak strength. These results demonstrate that ED bars in short tapered-cylindrical grouted connectors can perform similarly to bars with fully-embedded development lengths.

Keywords: Energy dissipating steel bars, Gap opening joints, Grouted seismic connectors, Precast concrete, Seismic, Type III connections

INTRODUCTION

Recently, a hybrid precast concrete wall^{1,2} with horizontal joints [Figures 1(a)-(b)] was validated as an ACI-318³ “special” shear wall following the requirements in ACI ITG-5.1.⁴ Precast building frames and bridge piers have also utilized similar systems. In the wall system that was validated, the base-panel-to-foundation joint is designed to undergo gap-opening displacements during a large earthquake. Ductile, Grade 60 ASTM A706⁵ deformed steel bars are provided across this gap-opening joint to yield and dissipate energy. The energy-dissipating (ED) bars are designed^{1,2} such that the tension steel strains at the maximum joint rotations are greater than $0.5\epsilon_{uel}$ (to provide adequate energy dissipation) but do not exceed $0.85\epsilon_{uel}$ (to prevent low-cycle fatigue fracture), where ϵ_{uel} is the monotonic strain capacity (i.e., uniform elongation strain) of the bar at peak strength, f_{uel} . A pre-determined length of each bar is unbonded (wrapped in a plastic sleeve) at the gap-opening joint so that the maximum steel strains remain below $0.85\epsilon_{uel}$.

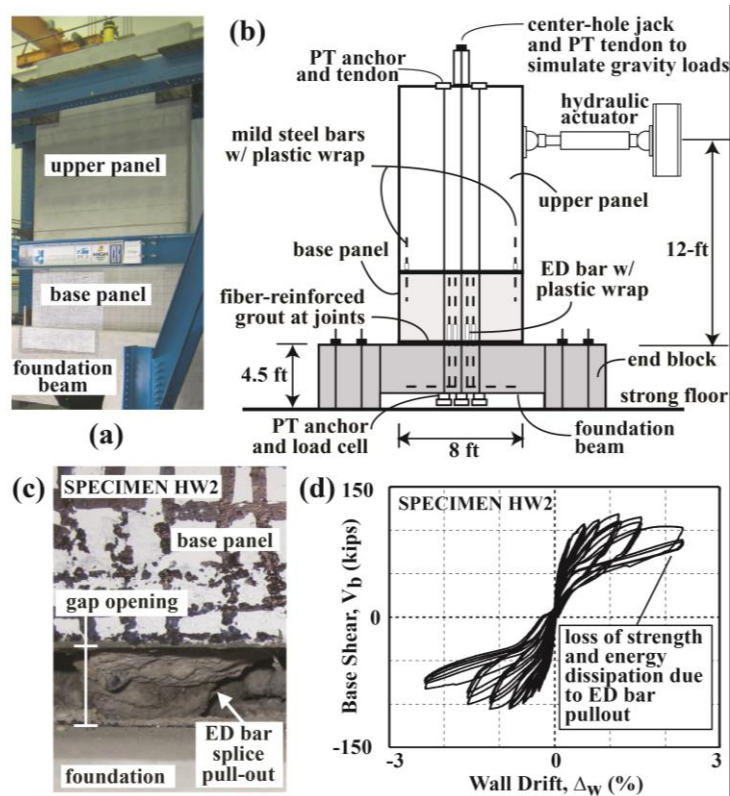


Figure 1. Hybrid walls:^{1,2} (a) photo; (b) elevation; (c) pullout in Specimen HW2; (d) measured behavior of Specimen HW2

If the expected steel strains are to be reached without pullout under cyclic loading, sufficient development length for the ED bars is required. In the hybrid precast wall system, this objective could only be achieved by casting (at one end) and grouting (at the other end) the full development length of the bars. Type II grouted splices in a similar wall (Specimen HW2) failed prematurely due to the pullout of the ED bars from the splices [Figure 1(c)], preventing validation of walls with Type II splices [Figure 1(d)]. These splices, which are

currently permitted by ACI ITG-5.2,⁶ met all ACI 318-14³ and AC133⁷ requirements and the grout for the splices met the splice manufacturer's specifications. The reason for the splice failures was because ED bars tested in precast walls per ACI ITG-5.1⁴ undergo greater strains and over a significantly larger number of cycles than the strain history required to classify a Type II splice per AC133.⁷ In accordance with the need for a higher-performing (Type III) connection for the ED bars, the current paper discusses the results from four ED bar specimens investigating the use of a new type of tapered-cylindrical grouted seismic connector.

TEST SETUP

The test setup used in the connection experiments is shown in Figure 2. The “foundation” and “wall panel” blocks were cast separately and then connected together using a single grouted Type III connector at the center. The foundation block (Figure 3), which had a width (thickness) of $t_f = 24$ in., height of $h_f = 36$ in., and length of $l_f = 54$ in., was designed to represent the foundation in a precast concrete wall system. The height of the block was designed to accommodate two ED bar connector sleeve ducts; one on top and one on bottom of the block. This allowed the foundation block to be reused in two separate tests by rotating the top of the block with the bottom. Grade 60 vertical and horizontal reinforcement was designed around each connector duct using a strut-and-tie model.

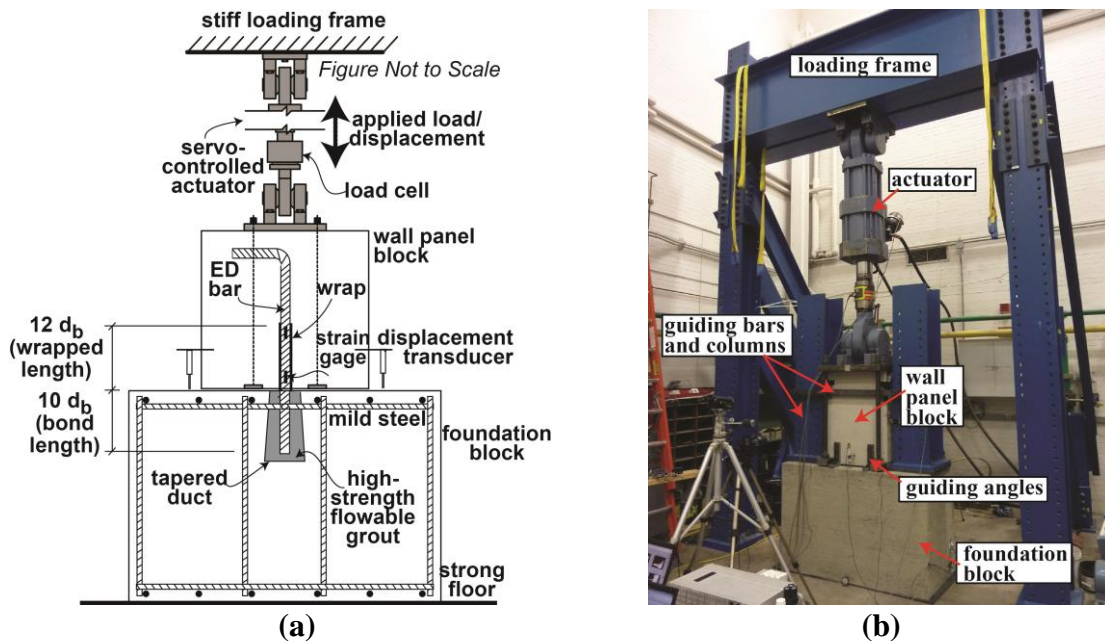


Figure 2. Test setup: (a) schematic; (b) photograph

The “wall panel” block (Figure 4), which had a width (thickness) of $t_w = 15$ in., height of $h_w = 32$ in., and length of $l_w = 24$ in., was designed to represent a slice over the length of a precast wall panel at the base. The Grade 60 mild steel reinforcement placed within the block was similar to that found around the ED bars in a typical hybrid precast wall base panel. A

No. 7 (nominal diameter, $d_b = 0.875$ in.) Grade 60 ASTM A706 reinforcing bar served as the ED bar to connect the wall panel and foundation blocks in all four tests. The ED bar was cast at the center of the wall panel block with a 90° hook to achieve full development at the top of the block (note that this hook would not be needed in a full-scale/full-height wall panel in practice). The bar was unbonded from the concrete over a length of $12d_b$ (10.5 in. for a No. 7 bar) at the bottom of the wall panel block by wrapping it inside a plastic sleeve. The unbonded portion of the ED bar, which is a typical feature to limit the maximum steel strains in hybrid precast systems, was long enough to: (1) result in significant elongation of the bar before fracture (therefore, allow measurable separation at the joint between the wall panel block and the foundation block); and (2) reduce the effect of any additional bar debonding (due to the cyclic loading of the bar) on the steel strains determined from the measured joint separation and the wrapped length.

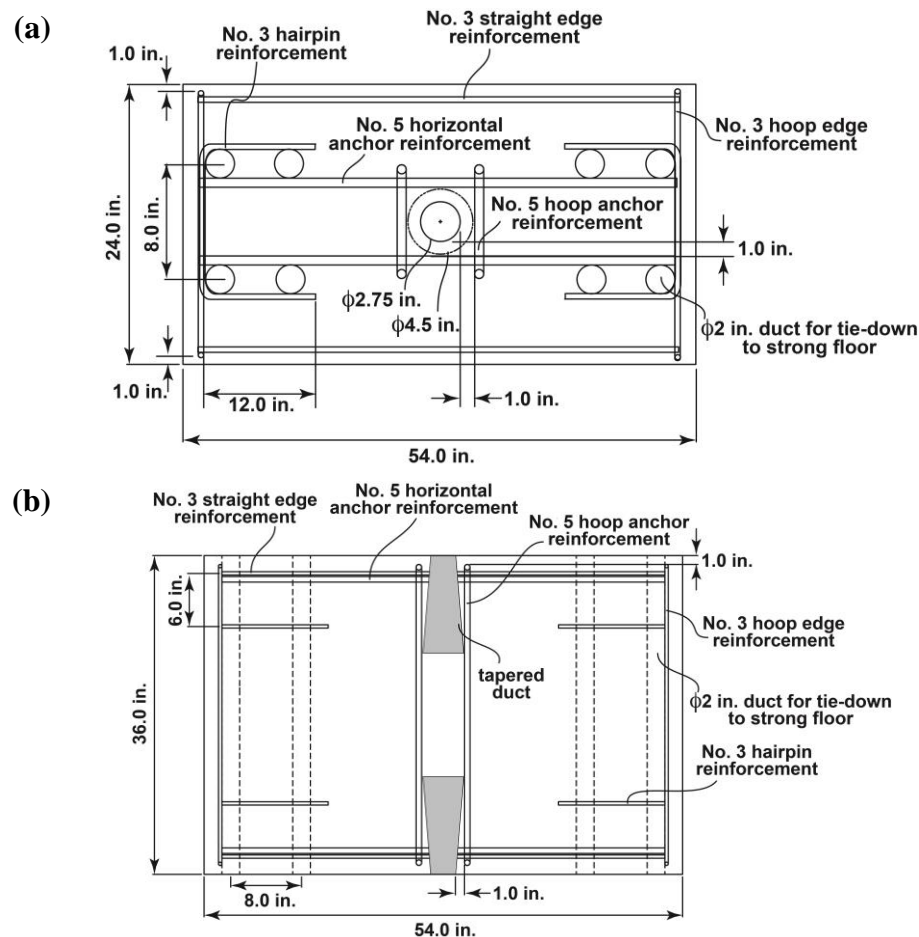


Figure 3. Foundation block details: (a) plan; (b) longitudinal elevation

During fabrication, the ED bar protruded out of the bottom of the wall panel block over the specified connection bond length. The cement-based high-strength flowable grout was mixed and placed manually up to a pre-determined depth from the top of the connector sleeve duct at the top of the foundation block. Then, the connection between the wall panel and foundation blocks was achieved by embedding the protruding length of the ED bar within the

grout inside the connector duct. The original grout depth inside the duct is a function of the ED bar size and the connector duct geometry, and was determined such that the grout cone would rise to the top of the connector sleeve upon embedment of the ED bar. To allow the ED bar to be loaded into a small amount of compression strain without the wall block coming into contact with the foundation block, a small initial gap was created (using 0.015 in. thick temporary shims) at the horizontal joint between the two blocks.

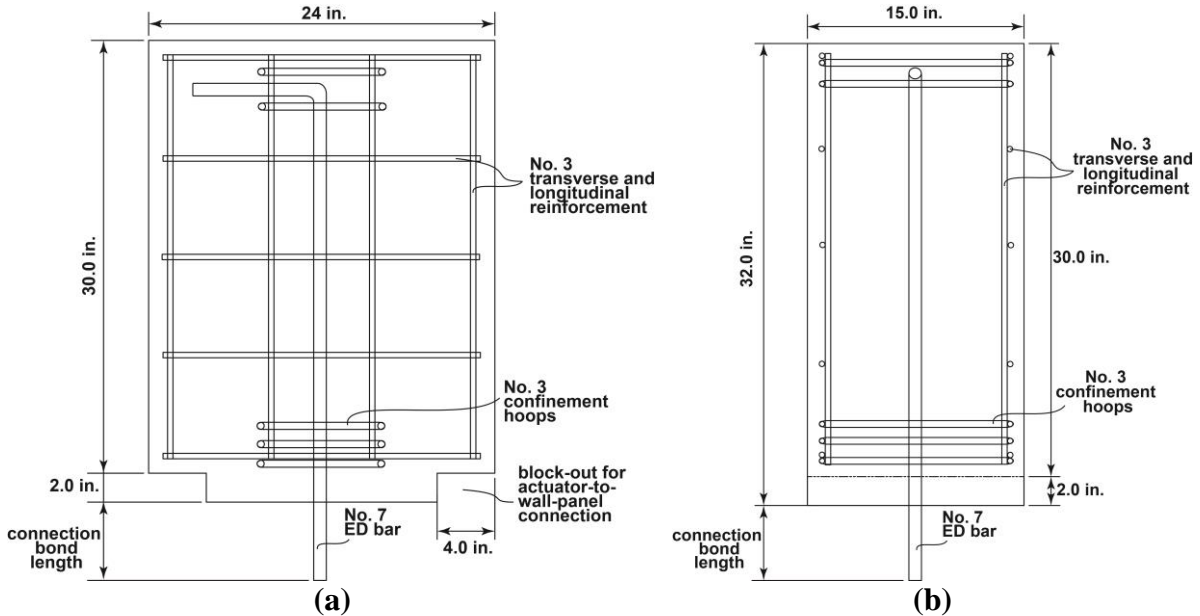


Figure 4. Wall panel block details: (a) longitudinal elevation; (b) transverse elevation

ED BAR CONNECTION PROPERTIES

The connector sleeve ducts used in the four tests are shown in Figure 5 and listed in Table 1. The sleeves were made by a local sheet metal manufacturer using light gauge (gauge 25) smooth sheet metal with a thickness of 0.0209 in. The ducts were slightly longer than the connection bond length of the ED bars for practical tolerance purposes. The duct taper entrance inner diameter was chosen so as to provide enough clearance and tolerance for the No. 7 ED bar. The same high-strength, cementitious grout product type was used in all four tests. For each connection, a 50-lb bag of prepackaged grout was mixed per manufacturer's instructions to reach a "flowable" consistency. The flow diameter (spread) of each batch was measured using a 2-in. diameter by 4-in. tall cylinder that was filled with grout and slowly lifted on top of a "flow template." The compression strength of the grout on the day of connection testing was determined from 2x2x2 in. grout cubes. Although a reasonably consistent grout spread diameter of 5 to 6 in. was achieved for the four connections, there were considerable differences in the grout strength as can be seen in Table 2.

The connector duct in Specimen 1-1 had a length of 11 in., taper angle of $\theta = 4.5^\circ$ (with taper entrance inner diameter of 2.75 in. and exit inner diameter of 4.5 in.), and a smooth (uncorrugated) surface. The bond length of the ED bar was $10d_b$ (8.75 in. for a No. 7 bar).

Specimen 1-2 investigated a longer bond length of $15d_b$ (13.125 in. for a No. 7 bar.). Surface corrugations (deformations) were placed at approximately 1 in. spacing at the bottom and top of the connector duct to provide additional mechanical interlock for the grout cone. The taper angle was kept at $\theta = 4.5^\circ$ (with taper entrance inner diameter of 2.75 in. and exit inner diameter of 5.25 in.). The duct length was increased to 15.75 in. to accommodate the longer ED bar bond length. The average connection test-day grout strength for this specimen (8,630 psi) was lowest out of the four specimens. Specimen 1-3 used a duct with the same dimensions as in Specimen 1-1; however, this duct had surface corrugations at approximately 1 in. spacing throughout its length. The ED bar bond length was kept at $10d_b$. A larger duct taper angle of $\theta = 9.0^\circ$ (with taper entrance inner diameter of 2.75 in. and exit inner diameter of 6.25 in.) was investigated in Specimen 1-4. Corrugations spaced at approximately 1 in. were also included on this duct. The average connection test-day grout strength for Specimen 1-4 (9,515 psi) was highest out of the four specimens.

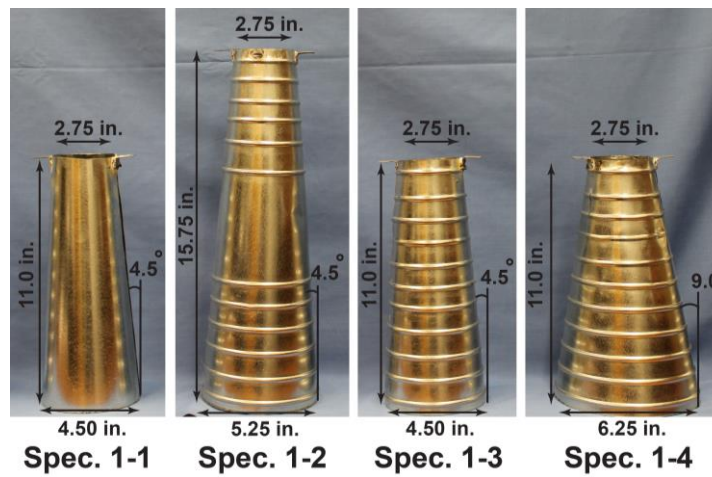


Figure 5. Connector sleeve ducts

Table 1: Connector duct and ED bar details

Spec. No.	Duct					ED Bar		
	Taper (deg.)	Entrance dia. (in.)	Exit dia. (in.)	Surface Corrugations	Length (in.)	Size	Wrapped Length (in.)	Bond Length (in.)
1-1	4.5	2.75	4.5	none	11	No. 7	10.5	8.75
1-2	4.5	2.75	5.25	spaced @ 1 in.	15.75	No. 7	10.5	13.125
1-3	4.5	2.75	4.5	spaced @ 1 in.	11	No. 7	10.5	8.75
1-4	9.0	2.75	6.25	spaced @ 1 in.	11	No. 7	10.5	8.75

Table 2: Connection grout details

Spec. No.	Grout Type	Average Test-Day Compression Strength (psi)	Test-Day Age (days)
1-1	cementitious*	9,500	54
1-2	cementitious*	8,630	124
1-3	cementitious*	8,965	135
1-4	cementitious*	9,515	41

*Identical product type from a single manufacturer was used in all four specimens

INSTRUMENTATION AND LOADING

As shown in Figure 2, the foundation block was fixed to the laboratory strong floor and the wall panel block was connected to a servo-controlled hydraulic actuator supported by a stiff steel loading frame. Four linear variable displacement transducers (LVDTs) were placed at mid-length along the four edges of the horizontal joint to measure the relative displacement between the wall panel and foundation blocks. Additionally, two strain gauges were placed on the wrapped length of the ED bar and eight strain gauges were used on the mild steel reinforcement around the connector duct in the foundation block. To determine the stress in the ED bar, the measured force in the hydraulic actuator was divided by the nominal bar area.

The strain gauges on the ED bar failed relatively early during each test; and thus, the LVDT displacements measured throughout the test were used to estimate the bar strains. The strain gauge data captured the initial stiffness and initial strains of the ED bar much better than the LVDTs, which tended to overestimate the initial bar strains. This could have been due to slightly greater joint separation at the LVDT locations along the four outer edges of the wall panel block as compared to the separation at the ED bar location at the center of the block. A possibly greater factor on the estimation of the ultimate steel strains from the LVDT displacements was the additional debonding that likely occurred at each end of the wrapped ED bar under the cyclic loading history. According to Smith and Kurama,¹ the total length of additional debonding expected to develop in an ED bar during cyclic loading to $0.85\epsilon_{uel}$ is approximately equal to $2d_b$ ($1d_b$ at each end of the wrapped region). The additional debonding length in bars subjected to pure axial loading (as in the testing of the ED bar connections herein) may be smaller than the debonding length in bars subjected to combined axial and lateral loads (as in the gap-opening base joint of the hybrid walls tested by Smith and Kurama¹). Furthermore, visual evidence after the completion of the ED bar connection tests indicated an additional debonding length of no more than $0.5d_b$ at the top of the foundation block. Since it was not possible to determine the amount of debonding inside the wall panel block, the same debonding length of $0.5d_b$ was assumed at both ends of the wrapped length. Thus, the bar strains were estimated by dividing the average displacement (i.e., relative joint displacement) from the four LVDTs with the total estimated unbonded length of $13d_b$ (i.e., $12d_b$ of wrapped length plus $1d_b$ of additional debonding). Even though the additional debonding likely developed gradually throughout each test, this “correction” was applied to the entire LVDT strain history since the property of most interest was the largest tension strains towards the end of the test.

During testing, the hydraulic actuator was used to move the wall panel block vertically to subject the ED bar to a rigorous quasi-static cyclic axial strain history. The strain history varied slightly between the four tests but was in general consistent with the recommended loading in Smith et al.² for the validation of ED bar connections in hybrid precast walls. As an example, Figure 6 shows the corrected LVDT strain history applied on Specimen 1-1 (green line). The bar was first subjected to 20 cycles reaching a maximum tension stress equal to about 95% of the measured monotonic yield strength, f_{sy} in tension and about 50% of f_{sy} in compression. Following these initial 20 cycles, 6 cycles were applied in each subsequent loading series, with the tension strain amplitude increased to approximately 3/2

times the strain amplitude from the previous series. After reaching the peak tension strain in each cycle, the loading was reversed up to a small amount of compression strain, thus subjecting the bar to stress reversal (simulating gap-closing along the joint). Testing continued until failure, with the objective of sustaining a maximum tension strain amplitude of $+0.85\epsilon_{uel}$ (or greater) over 6 cycles, or ductile fracture of the bar.

Also shown in Figure 6 is the required strain history to certify Type II splices per AC133⁷ (black dashed line). It can be seen that the strain history used in the current project was significantly more rigorous (both in amplitude and in number of cycles) than that required to certify Type II splices. The strain history of the grouted Type II ED bar splice that pulled out at a strain of $\epsilon_{su} = 0.021$ in./in. (approximately $0.14\epsilon_{uel}$) during the ACI ITG-5.1⁴ testing of hybrid wall Specimen HW2² is also shown in Figure 6 (red line). This result demonstrates that the Type II splice used in Specimen HW2 exceeded the cyclic demands prescribed by AC133,⁷ but the bar pulled out at a significantly smaller strain than that was needed for the ACI ITG-5.1⁴ validation of the wall.

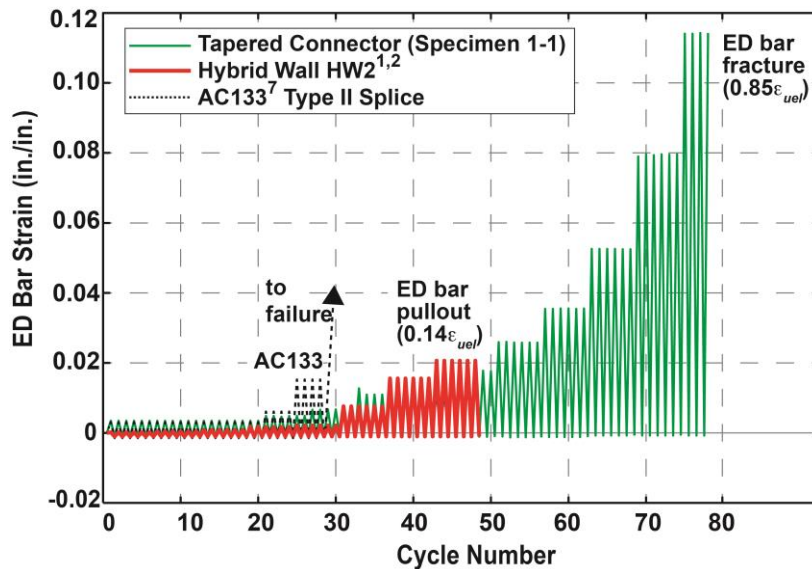


Figure 6. Corrected LVDT strain history in Specimen 1-1

TEST RESULTS

The results of the tests, including maximum tension strains, total number of loading cycles, number of cycles sustained in the last strain increment, and failure mode are listed in Table 3 and discussed in more detail below. Figures 7(a)-(d) (black lines) show the measured cyclic stress versus corrected LVDT strain behavior of the ED bar specimens. Also shown in these figures are the measured monotonic tension stress-strain behaviors of three bars from the same heat as the ED bars used in the connections. The bar strains in these monotonic tests were measured using an extensometer with a 2 in. gauge length. The resulting average monotonic strain capacity of the steel at peak strength, f_{uel} was found to be $\epsilon_{uel} = 0.1342$ in./in. (uniform elongation strain).

The ED bar in Specimen 1-1 [Figure 7(a)] achieved ductile low-cycle fatigue fracture (without pullout) during the 5th cycle of the final set of cycles to a maximum corrected LVDT strain of $\epsilon_{su} = 0.1143$ in./in. (approximately $0.85\epsilon_{uel}$), reaching the $0.85\epsilon_{uel}$ target. Since the connection duct in this first test was smooth, it was concluded that duct corrugations were not necessary and that the 4.5° taper angle provided adequate interlock to provide the desired performance. During load reversal into compression, there were some irregularities in the ED bar stress-strain behavior due to unintended rotation of the wall panel block with respect to the foundation block. The guiding columns and bars shown in Figure 2(b) were not present in the initial laboratory set-up. The observed rotation was likely because of a small misalignment of the wall panel block and ED bar with the actuator axis. As the wall panel block rotated, it came into contact with the foundation block along one edge while the other edges were not in contact. This is evident in the sudden increase in compression stiffness during the last cycles in Figure 7(a). Subsequently, the wall panel block rotated back to flat in between the guiding angles and the compression stiffness decreased because the wall panel block was no longer in contact with the foundation block. There was another increase in stiffness towards the end of the compression cycle, which was likely due to the wall panel block coming into contact with the small amount of grout that had bulged out from the connection.

Table 3: Cyclic performance of tested connectors

Specimen No.	Total No. of Cycles Endured	Strain Amplitude of Last Series, ϵ_{su}	No. of Cycles Sustained in Last Series	Mode of Failure
1-1	78	0.1143 ($0.85\epsilon_{uel}$)	4	fracture
1-2	68	0.0971 ($0.72\epsilon_{uel}$)	6	fracture
1-3	70	0.0961 ($0.72\epsilon_{uel}$)	6	ductile pullout
1-4	76	0.1145 ($0.85\epsilon_{uel}$)	2	fracture

Due to the aforementioned irregularities, the measured stress-strain behavior for Specimen 1-1 in Figure 7(a) does not reflect the true behavior of the ED bar in compression. Note however that the behavior of the bar in tension was not affected, except for potentially earlier fracture of the bar due to the bending that occurred during the rotation of the wall panel block in compression. No deterioration of the concrete was observed around the grouted ED bar connection in the foundation block (see Figure 8). There was a slight bulging-out/deterioration of the grout at the top of the connection duct, but this did not affect the performance of the connection, other than an increase in the total unbonded length of the bar as discussed previously. Figure 9(a) shows the bar fracture from Specimen 1-1 as well as the grout-bulging that was observed. No damage was visible on the wall panel concrete, except for a small amount of crushing at the concrete edge where contact occurred with the foundation block during the unintended rotations of the wall panel block.

Following the testing of Specimen 1-1, the laboratory setup was modified by placing guiding columns and bars to prevent any significant rotation of the wall panel block. The smooth cyclic stress-strain behavior for Specimen 1-2 in Figure 7(b) verifies that the rotation of the wall panel was essentially eliminated. The ED bar achieved ductile fracture (without pullout)

during the 1st cycle after a complete set of 6 cycles to a maximum corrected LVDT strain of $\epsilon_{su} = 0.0971$ in./in. (approximately $0.72\epsilon_{uel}$). The fracture strain capacity of $0.72\epsilon_{uel}$ of this bar indicates that the maximum allowable strain of $0.85\epsilon_{uel}$ recommended for the design of ED bars in ACI ITG-5.2⁶ may be unconservative. Similar to Specimen 1-1, there was very little deterioration in or around the tapered-cylindrical connection, with only a slight bulging-out of the grout at the top of the connection duct. No other damage was visible.

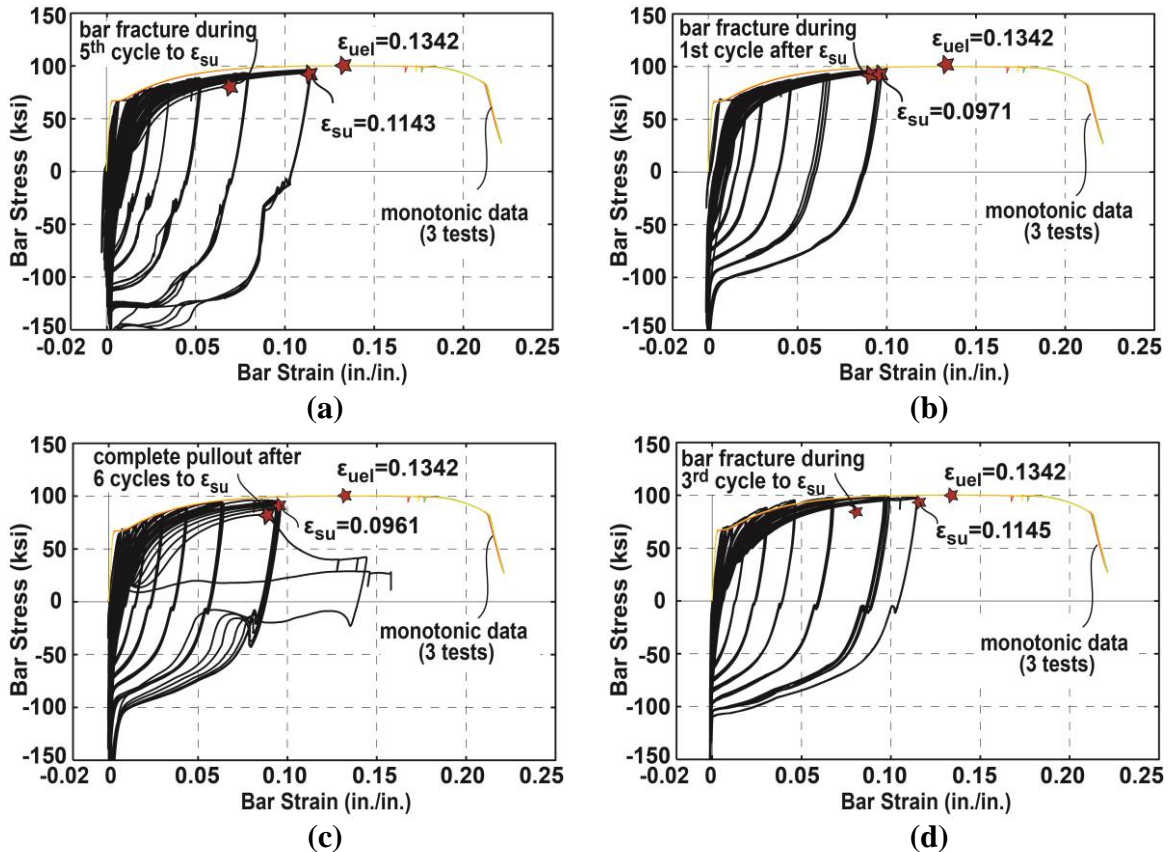


Figure 7. ED bar stress versus corrected LVDT strain behavior: (a) Specimen 1-1; (b) Specimen 1-2; (c) Specimen 1-3; (d) Specimen 1-4

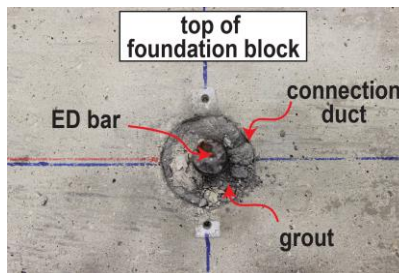


Figure 8. Top of foundation block after testing (Specimen 1-1)

Figure 7(c) shows the measured cyclic stress-strain behavior for Specimen 1-3, which was similar to Specimen 1-1 except for the slightly lower compression strength of the connection

grout (Table 2) and the presence of duct corrugations. The ED bar in Specimen 1-3 experienced progression of pullout during the loading cycles to a corrected LVDT strain of $\varepsilon_{su} = 0.0961$ in./in. (approximately $0.72\varepsilon_{uel}$), with the development of complete pullout [bond failure; see Figure 9(b)] after the completion of 6 cycles at this strain level. This bond failure occurred in a ductile manner after significant nonlinear straining of the bar as shown in Figure 7(c), but at a smaller strain than the $0.85\varepsilon_{uel}$ target. Since the bond failure occurred between the bar and the surrounding grout, the corrugations on the connector duct surface were not effective. These results demonstrate the importance of the grout strength in determining the failure mode of the ED bar and the resulting strain capacity.

Specimen 1-4 investigated a larger connection duct taper angle of $\theta = 9.0^\circ$. As shown in Figure 7(d), the ED bar achieved ductile fracture (without pullout) during the 3rd cycle of the final set of cycles to a maximum corrected LVDT strain of $\varepsilon_{su} = 0.1145$ in./in. (approximately $0.85\varepsilon_{uel}$). No bulging of the grout cone from the top of the connector duct was visible during or after the test, which may indicate that the increased taper angle was more effective in confining the grout cone inside the connection. However, since the larger taper angle results in a larger connector, the taper angle of 4.5° was deemed more practical while still providing the desired connection performance.

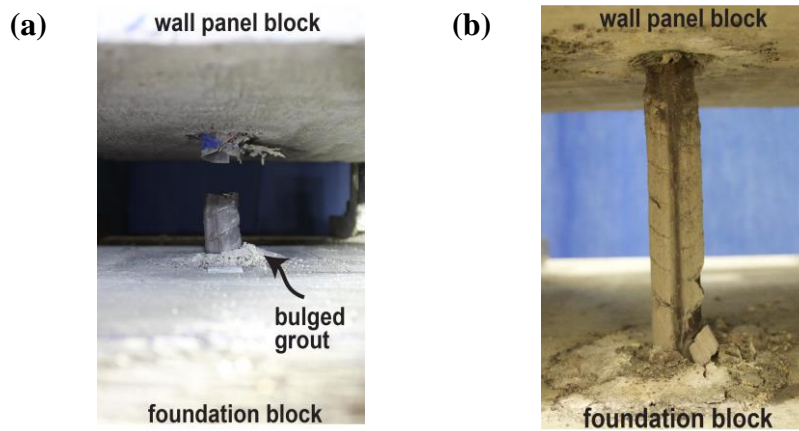


Figure 9: Failure modes: (a) bar fracture (Specimen 1-1); (b) bar pullout (Specimen 1-3)

SUMMARY AND ONGOING WORK

This paper presents the results from four test specimens on the quasi-static cyclic axial load behavior of a novel tapered-cylindrical cementitious grouted connection for energy dissipating (ED) deformed steel bars at gap-opening joints in seismic precast concrete structures. All four specimens failed in a ductile manner after sustaining rigorous cyclic loading to maximum bar strains ranging between $0.72\varepsilon_{uel}$ and $0.85\varepsilon_{uel}$ developed over a short grouted bond length (where, ε_{uel} is the monotonic strain capacity of the bar at peak stress). These results demonstrate that tapered-cylindrical grouted connectors have the capacity to develop ED bars up to the large cyclic strain demands expected at gap-opening joints in high

seismic regions. One specimen with slightly lower connection grout strength experienced ductile bond failure at the bar-to-grout interface. The other three specimens were able to achieve ductile low-cycle fatigue fracture of the ED bar. The following conclusions can be made based on the results from these initial four tests: (1) surface corrugations are not needed for the tapered connector sleeve ducts; (2) connection grout strength is very important in determining the failure mode of the ED bar and the resulting strain capacity; (3) a bond length of 10 times the nominal bar diameter (i.e., $10d_b$) is adequate to reach large cyclic bar strains; (4) although the tested connector taper angle of 9.0° resulted in less grout bulging from the sleeve duct, the smaller 4.5° taper angle is deemed more practical while still providing the desired connection performance; and (5) one of the specimens experienced low-cycle fatigue fracture after sustaining a maximum strain of approximately $0.72\varepsilon_{uel}$, which indicates that the maximum allowable strain of $0.85\varepsilon_{uel}$ recommended for the design of ED bars in ACI ITG-5.2⁶ may be unconservative. Note that these conclusions may be limited to the specimens and materials tested to date. Additional tests to be conducted in the near future will further investigate the effect of grout strength (especially lower grout strengths), ED bar size (diameter), connector duct taper angle, connector edge distance, and construction tolerances and inaccuracies.

ACKNOWLEDGEMENTS

This paper is based upon work supported by a Precast/Prestressed Concrete Institute (PCI) Daniel P. Jenny Research Fellowship and by a National Science Foundation Graduate Research Fellowship under Grant No. DGE-1144468. The authors acknowledge the support of the PCI Research and Development Council, the PCI Central Region, as well as the members of the Project Advisory Panel, who include Don Meinheit (chair) - Wiss, Janney, Elstner Associates; Ned Cleland - Blue Ridge Design; Tom D'Arcy - Consulting Engineers Group; David Dieter - Mid-State Precast; Sameh El Ashri - e.construct, Dubai; S.K. Ghosh - S.K. Ghosh Associates; Harry Gleich - Metromont Corporation; Neil Hawkins - Univ. of Illinois at Urbana-Champaign, IL; Walter Korkosz - Consulting Engineers Group; and Larbi Sennour - Consulting Engineers Group. Any opinions, findings, and conclusions or recommendations expressed in the paper are those of the authors and do not necessarily reflect the views of the individuals and organizations acknowledged above.

REFERENCES

1. Smith, B., Kurama, Y., "Seismic Design Guidelines for Special Hybrid Precast Concrete Shear Walls," Report NDSE-2012-02, University of Notre Dame, 2012. (*available at hybridwalls.nd.edu/Project/Downloads/Design_Guidelines.pdf*).
2. Smith, B., Kurama, Y., McGinnis, M., "Hybrid Precast Wall Systems for Seismic Regions," Report NDSE-2012-01, University of Notre Dame, 2012. (*available at hybridwalls.nd.edu/Project/Downloads/Final_Report.pdf*).
3. ACI, "Building Code Requirements for Structural Concrete (ACI 318-14) and Commentary (ACI 318R-14)," ACI Committee 318, American Concrete Institute, 2014.

4. ACI, “Acceptance Criteria for Special Unbonded Post-Tensioned Precast Structural Walls Based on Validation Testing and Commentary (ACI-ITG-5.1),” Innovation Task Group 5, American Concrete Institute, 2007.
5. ASTM A706/A706M-14, “Standard Specification for Deformed and Plain Low-Alloy Steel Bars for Concrete Reinforcement,” ASTM International, West Conshohocken, PA, 2014. (*available from www.astm.org*).
6. ACI, “Requirements for Design of a Special Unbonded Post-Tensioned Precast Shear Wall Satisfying ACI ITG-5.1 and Commentary (ACI ITG-5.2),” Innovation Task Group 5, American Concrete Institute, 2009.
7. ICC, “Acceptance Criteria for Mechanical Connector Systems for Steel Reinforcement Bars,” AC133, ICC Evaluation Service, 2010.